

# Current State Art of Hot Thermocouple Technology—Novel Way for the Study of Mold Flux High-Temperature Properties

Lei Zhang, Wanlin Wang and Lejun Zhou

**Abstract** Hot Thermocouple Technology has been developed and approved to be a novel method to study the high-temperature related properties of molten slag. In this study, it will first give the development of Hot Thermocouple Technology, and its typical application to the mold flux. One example of crystallization process of the mold flux for casting low carbon (LC flux) and medium carbon steels (MC flux) were investigated by using Double Hot Thermocouple Technology (DHTT). The results of LC flux showed that, the glass phase firstly formed at the low temperature side; then, the fine crystals precipitated at the liquid/glass interface and grew toward glass and later on to liquid phase. However, the crystals directly formed at the low temperature side when MC flux was under cooling process and grew toward the high temperature side; which indicated the crystallization ability of MC flux was stronger than LC flux. Another crystallization sample of CaO-SiO<sub>2</sub>-B<sub>2</sub>O<sub>3</sub> based fluoride-free mold flux (F-free flux) was studied by using Single Hot Thermocouple Technology (SHTT), and the results showed the crystals first precipitated in the middle of sample and moved toward the thermocouple side, then the precipitated crystals grew up and new crystals formed in the middle of sample and moved toward the side, until the crystallization was completed and reached a steady state; the crystallization mechanism of the F-free flux was 1-dimensional growth.

**Keywords** Double hot thermocouple technology · Single hot thermocouple technology · Mold flux · Crystallization

## Introduction

Mold flux plays an important role in the process of continuous casting, protecting the molten steel from oxidation, absorbing inclusions, providing the thermal insulation, lubricating the strand and controlling heat transfer between the mold and

---

L. Zhang · W. Wang (✉) · L. Zhou  
School of Metallurgical Science and Engineering, Central South University,  
Changsha 410083, People's Republic of China  
e-mail: Wanlin.Wang@gmail.com

© The Minerals, Metals & Materials Society 2018  
The Minerals, Metals & Materials Society, *TMS 2018 147th Annual Meeting*  
& *Exhibition Supplemental Proceedings*, The Minerals, Metals & Materials Series,  
[https://doi.org/10.1007/978-3-319-72526-0\\_19](https://doi.org/10.1007/978-3-319-72526-0_19)

201

steel shell [1–4]. Among them, the heat transfer ability of mold flux directly determines the surface defects of as-cast slabs. Uneven heat transfer in the mold and rapid cooling can cause enormous thermal stress on the initial shell, introducing corner cracks, longitudinal face cracks, depressions, and other surface defects [5, 6]. In order to minimize stresses, the horizontal heat transfer from molten steel through mold flux film to water-cooled copper mold should be uniformly controlled to achieve a thin and uniform partially solidified shell. Mold flux crystallization is known to inhibit radiative heat from the steel and can create air gaps between the mold and partially solidified shell during the initial solidification of molten steel [7, 8], which increases the interfacial thermal resistance. Since a thick crystalline layer can resist the in-mold ferrostatic pressure [9]; it is usually achieved by improving the crystallization ability of mold flux to maintain a thick solid crystalline layer of slag film. Thus, the research on the crystallization of mold flux is a key parameter in the process of continuous casting.

A variety of methods have been used to determine crystallization property of mold flux. Differential Thermal Analysis (DTA) is the most common method for studying the crystallization of mold flux. In this case, the slag sample together with a reference substance is melted in a furnace and then cooled, the heat generation or heat absorption will take place when the sample occurs physiochemical reactions, then the temperature difference between the sample and the reference material will occur and be recorded. But, the method is limited to direct observation of the solidification phenomena and their accuracy as the heat change is easy to be affected by many environmental factors. Another technique is also frequently employed to determine the crystallization behavior of mold flux, which the slag sample is placed inside a metallic mold and heated at the temperature up to melting point of the mold flux for melting and then quenched [10–12]. After solidification, the sample can be tested at room temperature by Scanning Electron Microscope (SEM) and X-ray diffraction (XRD) to analyze the proportion of crystalline and the type of the crystalline phases. However, the technique also can not observe in situ the crystallization process of mold flux and does not provide a quantitative measurement to characterize the slag crystallization behavior.

To properly characterize the evolution process of crystallization, the crystal morphology and crystal growth rates, etc. The technique which combines hot thermocouple technique with video observation and image analysis was successfully developed in 1950s by Ordway [13] and Welch et al. [14]. Based on this, Ishii and Kashiwaya developed the double hot thermocouple method and applied to a microgravity experiment to determine the microstructural change of a superconducting oxide in 1992 [15–17]. And the double hot thermocouple technology first was applied in the research area of mold flux in 1995 [18, 19], from then it has been widely used to study the high-temperature properties of mold flux subsequently. In this paper, the crystallization process of mold flux for casting low carbon (LC flux) and medium carbon steels (MC flux) were investigated by using Double Hot Thermocouple Technology (DHTT) and the crystallization mechanism of the

CaO-SiO<sub>2</sub>-B<sub>2</sub>O<sub>3</sub> based fluoride-free mold flux (F-free flux) was also studied by Single Hot Thermocouple Technology (SHTT).

## Experimental Apparatus and Method

### *Sample Preparation*

The chemical compositions of the LC flux and MC flux and F-free flux are listed in Table 1. All samples were prepared from reagent grade chemicals of CaO, SiO<sub>2</sub>, Li<sub>2</sub>O, CaF<sub>2</sub>, B<sub>2</sub>O<sub>3</sub>, and mechanical mixed prior to the placement inside the induction furnace, then it was heated to the melting point and held for 5 min to obtain a homogeneous melt. The molten slag was quickly poured onto a water-cooled copper plate to quench. The quenched samples were crushed and ground into powder samples for subsequent DHTT and SHTT experiments.

### *DHTT Experiments*

The crystallization experiments of the mold flux for casting LC and MC steels were conducted by using DHTT, and the DHTT apparatus as shown in Fig. 1. Figure 1a is the illustration of DHTT, where is two B-type thermocouples (CH-1 and CH-2), and a desired temperature gradient between the two thermocouples can be achieved through controlling the temperature of each thermocouple separately. Meanwhile, the images of mold flux crystallization are observed through a microscope and recorded by a connected CCD onto a DVD.

For the DHTT experiments, the mold flux sample was first mounted on one of the two thermocouples; then, it was melted at 1773 K (1500 °C) with a rate of 15 K/s. After eliminating bubbles and homogenizing its chemical composition for 180 s, the mold flux was stretched to 2 mm by the two thermocouples. Then, the temperature of CH-2 was directly quenched with the maximum rate of 30 K/s to 1073 K (800 °C) to achieve the desired thermal gradient for the crystallization. The temperature controlling profile for the DHTT experiments is shown in Fig. 2.

**Table 1** Chemical compositions of the mold fluxes after pre-melting (in Mass Pct)

	CaO/SiO <sub>2</sub> (C/S)	CaO	SiO <sub>2</sub>	Na <sub>2</sub> O	Li <sub>2</sub> O	CaF <sub>2</sub>	B <sub>2</sub> O <sub>3</sub>
LC flux	0.81	33.79	41.54	9.20	0.49	5.89	–
MC flux	1.32	43.51	32.86	5.11	0.5	3.92	–
F-free flux	1.15	41.80	36.38	7.97	2	–	5.83

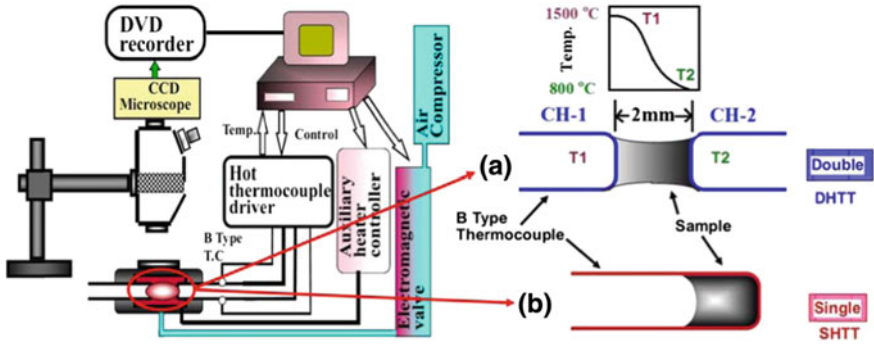
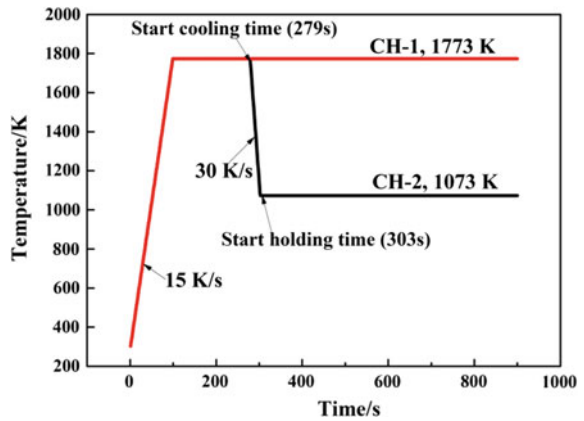


Fig. 1 The schematic of DHTT apparatus: a double and b single hot thermocouples

Fig. 2 The temperature controlling profile for DHTT experiments

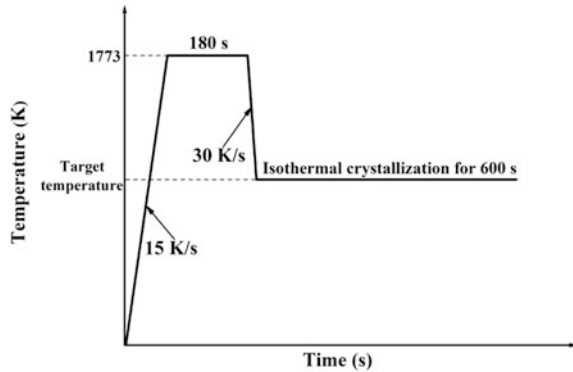


### SHTT Experiments

The crystallization mechanism of F-free flux was studied using SHTT, and the SHTT apparatus also as shown in Fig. 1. Figure 1b shows the schematic illustration of the SHTT, where is one of the two thermocouples, and the control of the temperature can be achieved through the corresponding auxiliary heater controller and its real-time temperature is recorded simultaneously. Also, the images of mold flux crystallization are observed through a microscope and recorded by a connected CCD onto a DVD.

For the SHTT experiments, the mold flux sample was first mounted on one thermocouple; and the sample was heated from room temperature to 1773 K at a rate of 15 K/s and held for 180 s to homogenize the chemical composition and minimize bubbles. Then, the molten slag was cooled at a rate of 30 K/s to various target temperatures to observe the isothermal crystallization for 600 s. The temperature controlling profile for the SHTT experiments is shown in Fig. 3.

**Fig. 3** The temperature controlling profile for SHTT experiments



## Results and Discussion

### *The Evolution Crystallization Process of LC Flux and MC Flux for DHTT Experiments*

Figure 4 shows the snapshots of the evolution crystallization process of LC flux for DHTT experiment. It can be seen that the mold flux is complete melted and is liquid when the two thermocouples are at 1773 K (Fig. 4a); then, the temperature of CH-1 thermocouple is kept 1773 K, while the temperature of CH-2 thermocouple is cooled to 1073 K with the rate of 30 K/s, this moment the mold flux near CH-1 side still as liquid and the mold flux near CH-2 side transform to glass phase (Fig. 4b); when the holding time reaches 82 s, some fine crystals precipitate at the liquid/glass interface, as shown in Fig. 4c; with time goes on, some dendritic crystals form in the middle of liquid mold flux and grow toward CH-1 side, as shown in Fig. 4d–g; when the holding time reaches 556 s, the crystallization is finished and the structure of the whole mold flux step into a relative steady state, where a little mold flux near CH-1 side is liquid and a little mold flux near CH-2 side is glassy phase and the others are crystal phase (Fig. 4h). It can be concluded from the whole process that the incubation time of the LC flux is about 82 s and the complete crystallization time is about 556 s.

The snapshots of the crystallization evolution process of MC flux for DHTT experiment are shown in Fig. 5. It can be observed that the whole mold flux as liquid when the both thermocouples are at 1773 K (Fig. 5a); then, the dendritic crystals begin to precipitate near the CH-2 side during the cooling process of CH-2 (Fig. 5b); later on, the crystals grow from the low temperature CH-2 side to high temperature CH-1 side, as shown in Fig. 5c–e; and some crystals precipitate near the CH-1 side and grow toward the middle (Fig. 5f–g); after the crystallization time keeps 49 s, the crystallization is completed and reaches a steady state, where a little liquid mold flux near CH-1 side and the others are crystal phase and no glass phase.

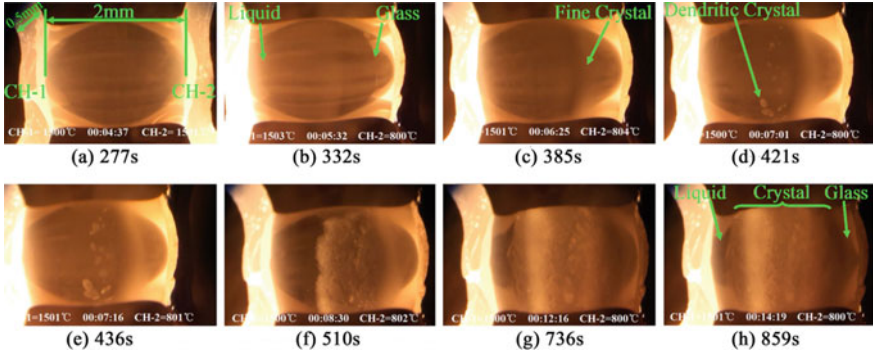


Fig. 4 The evolution process crystallization of LC flux for DHTT experiment [20]

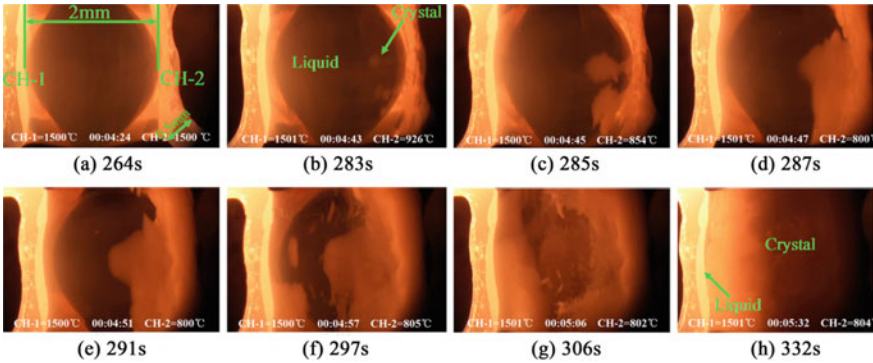


Fig. 5 The evolution process crystallization of MC flux for DHTT experiment [20]

It can be concluded from the whole process that the incubation time of the MC flux is about 0 s and the complete crystallization time is about 49 s.

Comparing with LC flux, the thickness of the MC flux crystal layer is thicker than LC flux, and the growth rate of MC flux crystal is much faster than LC flux. It indicates that the crystallization ability of MC flux is stronger than LC flux.

### *The Crystallization Mechanism of F-free Flux for SHTT Experiments*

Figure 6 shows the snapshots of the evolution crystallization process of F-free flux at 1673 K (1400 °C) for isothermal crystallization using SHTT. It can be observed that the incubation time of F-free flux is 72 s and the complete crystallization time is about 156 s. The crystals first precipitate in the middle of sample and move

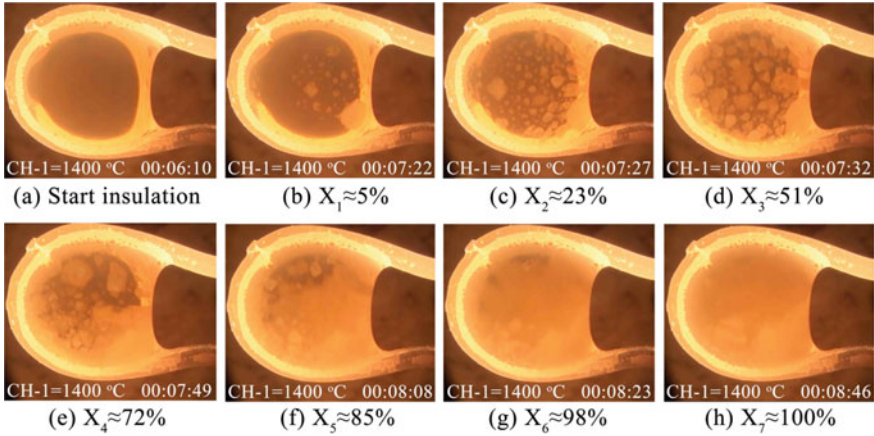


**Fig. 6** The evolution process crystallization of F-free flux for SHTT experiment

toward the side. With the holding time goes on, the precipitated crystals grow up and meantime new crystals continue to precipitate in the middle and move toward the side of sample. Thus, the crystal volume fraction is becoming larger, until the crystallization is completed and reaches a steady state.

In order to study the crystallization mechanism of F-free flux, the Johnson-Mehl-Avrami (JMA) model [21, 22] need be applied in this work. According to the JMA model, the volume fraction of crystals ( $X$ ) is given by

$$X = 1 - \exp\{-[k(t - \tau)]^n\} \quad (1)$$

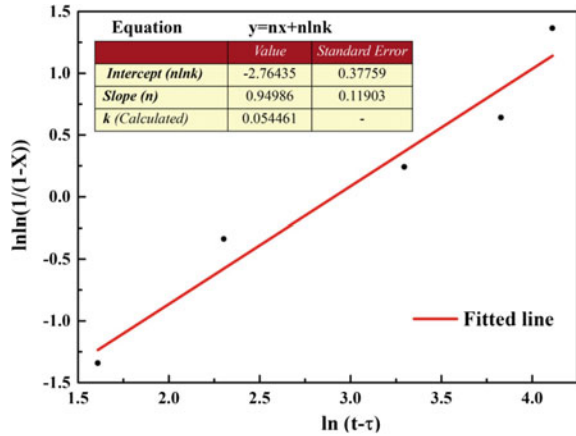
where  $t$  is the crystallization time,  $\tau$  is the incubation time,  $k$  is the constant of effective crystallization rate (including both nucleation and growth), and  $n$  is the Avrami exponent associated with nucleation and growth mechanism. The volume fraction of crystallization ( $X$ ) obtained at a certain temperature was defined as  $X = A_c/A_T$ , where  $A_c$  is the area of the crystal and  $A_T$  is the total area of the mold flux. The values of  $X$  have been obtained by the above image analysis and shown in Fig. 6.

Therefore, the values of  $n$  and  $k$  can be determined according to the following equation by rearranging Eq. (1) into Eq. (2).

$$\ln\ln(1/1 - X) = n\ln k + n\ln(t - \tau) \quad (2)$$

$k$  and  $n$  can be acquired by plotting  $\ln\ln(1/(1-X))$  versus  $\ln(t-\tau)$ , where  $n$  and  $k$  can be obtained from slope and intercept of the fitted line, respectively. The plots of  $\ln[\ln(1/(1-X))]$  as a function of  $\ln(t-\tau)$  and where  $n$  and  $k$  can be obtained are shown in Fig. 7. According to the corresponding relationship between  $n$  and the crystallization mechanism was given out by Christian [23], the value of  $n$  is about 1 indicates the crystallization mechanism of F-free flux is 1-dimensional growth.

**Fig. 7** The relation of crystal volume fraction evolution with function of time for F-free flux



## Conclusions

In this paper, the development of Hot Thermocouple Technology has been introduced, and also crystallization process of the mold flux for casting low carbon (LC flux) and medium carbon steels (MC flux) by using Double Hot Thermocouple Technology (DHTT) and the crystallization mechanism of fluoride-free mold flux by using Single Hot Thermocouple Technology (SHTT) have been systematically studied. The main conclusions are summarized as follows:

- (1) In the crystallization process of LC flux, the glass phase first formed when the CH-2 was quenched to 1073 K (800 °C) with the cooling rate of 30 K/s. Then, the fine crystal particles precipitated at the liquid/glass interface and grew toward the glass. The dendritic crystals later formed in the middle of the mold flux and grew toward the hot side. And the incubation time was about 82 s and the complete crystallization time was about 556 s.
- (2) During the crystallization process of MC flux, the crystals formed directly near the CH-2 side during the cooling process of the CH-2 thermocouple. Then crystals began to precipitate near the CH-1 side and grew to the middle. The incubation time and the complete crystallization time was about 0 s and 49 s, individually. Comparing with LC flux, the thickness of the MC flux crystal layer was thicker than LC flux, and the growth rate of MC flux crystals was much faster than LC flux.
- (3) The evolution crystallization process of F-free flux showed the crystals first precipitated in the middle of sample and moved toward the side, then the precipitated crystals grew up and new crystals formed and moved toward the side, until the crystallization was completed and reached a steady state. The results of crystallization kinetics indicated the crystallization mechanism of F-free flux was 1-dimensional growth.



## References

1. Zhou LJ, Wang WL et al (2012) A kinetic study of the effect of basicity on the mold fluxes crystallization. *Metall Mater Trans B* 43(2):354–362
2. Mills KC, Fox AB, Li Z, Thackray RP (2005) Performance and properties of mould fluxes. *Ironmak Steelmak* 32(1):26–34
3. Wang WL, Cramb AW (2005) The observation of mold flux crystallization on radiative heat transfer. *ISIJ Int* 45(12):1864–1870
4. Yamauchi A, Sorimachi K, Sakuraya T, Fujii T (1993) Heat transfer between mold and strand through mold flux film in continuous casting of steel. *ISIJ Int* 33(1):140–147
5. Li C, Thomas BG (2004) Thermomechanical finite-element model of shell behavior in continuous casting of steel. *Metall Mater Trans B* 35(6):1151–1172
6. Sridhar S, Mills KC, Mallaband ST (2002) Powder consumption and melting rates of continuous casting fluxes. *Ironmak Steelmak* 29(3):194–198
7. Gu K, Wang WL, Zhou LJ et al (2012) The effect of basicity on the radiative heat transfer and interfacial thermal resistance in continuous casting. *Metall Mater Trans B* 43(4):937–945
8. Wang WL, Cramb AW (2010) Study of the effects of the mold surface and solid mold flux crystallization on radiative heat transfer rates in continuous casting. *Steel Res Int* 81(6):446–452
9. Wei J, Wang WL et al (2014) Effect of  $\text{Na}_2\text{O}$  and  $\text{B}_2\text{O}_3$  on the crystallization behavior of low fluorine mold fluxes for casting medium carbon steels. *Metall Mater Trans B* 45(2):643–652
10. Hering L, Heller HP, Fenzke HW (1992) Investigations for flux power selection in slab continuous-casting. *Stahl Und Eisen* 112(8):61–65
11. Sakai H, Kawashima T, Shiomi T, Watanabeand K, Iida T (1997) Molten the interface. In: The final step involves the dissolution of the Slags, Slags and Salts'97 Conference, Warrendale, PA
12. Bhamra M, Charlesworth M, Wong S, Sawyers VD, Cramb AW (1996). In: 54th Electric Furnace Conference, Dallas, TX, 9–12 Dec 1996
13. Ordway F (1952) Techniques for growing and mounting small single crystals of refractory compounds. National Bureau of Standards
14. Welch JH (1954) A simple microscope attachment for observing high-temperature phenomena. *J Sci Instrum* 31(12):458
15. Kuranaga T, Kashiwaya Y, Ishii K (1995). In: International Symposium on Advanced Materials and Technology for 21st Century. JIM'95 Fall Meeting, Honolulu
16. Scholze H (1991) Glass: Nature. Structure and properties. Springer, Berlin
17. Uhlman DR (1983) Glass formation, a contemporary view. *J Am Ceram Soc* 66(2):95–100
18. Kashiwaya Y, Cicutti CE et al (1998) Development of double and for in situ observation and single hot thermocouple technique measurement of mold slag crystallization. *ISIJ Int* 38(4):348–356
19. Kashiwaya Y, Cicutti CE, Cramb AW (1998) An investigation of the crystallization of a continuous casting mold slag using of the single hot thermocouple technique. *ISIJ Int* 38(4):357–365
20. Zhou LJ, Wang WL, Huang DY et al (2012) In situ observation and investigation of mold flux crystallization by using double hot thermocouple technology. *Metall Mater Trans B* 43(4):925–936
21. Sun NX, Liu XD, Lu K (1996) An explanation to the anomalous avrami exponent. *Scripta Mater* 34:1201–1207
22. Wang WL (2007) PhD thesis, Carnegie Mellon University
23. Christian JW (2002) The theory of transformations in metals and alloys, 3rd edn. Pergamon Press Ltd, London, UK